Leveraging Quantitative Analysis for Severity Assessment of Knee Osteoarthritis

Asif Ihtemadul Haque
Computer Science and Engineering
Bangladesh University of Engineering and Technology
Dhaka, Bangladesh
asifihtemadulhaque@gmail.com

Shamim-Al Mamun
Computer Science and Engineering
Bangladesh University of Engineering and Technology
Dhaka, Bangladesh
1805060@cse.buet.ac.bd

Sanjana Binte Siraj
Computer Science and Engineering
Bangladesh University of Engineering and Technology
Dhaka, Bangladesh
0424052050@cse.buet.ac.bd

Tanvir R. Faisal
Mechanical Engineering
University of Louisiana at Lafayette
Lafayette, Louisiana, USA
tanvir.faisal@louisiana.edu

Mahmuda Naznin
Computer Science and Engineering
Bangladesh University of Engineering and Technology
Dhaka, Bangladesh
mahmudanaznin@cse.buet.ac.bd

Abstract

Knee Osteoarthritis (KOA) is a major cause of disability all over the world. For severity assessment, a popular qualitative method is Kellgren-Lawrence (KL) grading which varies from human to human. If quantification is added, it will provide an automated and correct picture of the KOA severity level. In this research, we have measured the joint space between the tibia and femur for each grade of osteoarthritis. By identifying the percentage range of joint space width for osteoarthritic knee joints, we have developed a method to aid in decision-making for advanced diagnosis and treatment. The proposed framework achieved an accuracy of 82.96% in KOA detection, demonstrating its efficiency and suitability for low-resourced clinical settings.

ACM Reference Format:
Asif Ihtemadul Haque, Shamim-Al Mamun, Sanjana Binte Siraj, Tanvir R. Faisal, and Mahmuda Naznin. 2025. Leveraging Quantitative Analysis for Severity Assessment of Knee Osteoarthritis. In *12th International Conference on Next Generation Computing, Communication, Systems and Security (NSysS '25), December 18–20, 2025, Sylhet, Bangladesh.* ACM, New York, NY, USA, 8 pages. https://doi.org/10.1145/3777555.3777566

1 Introduction

Knee Osteoarthritis (KOA) is a significant global health concern, with an estimated million individuals (aged 40 years and older) affected globally in 2020. The prevalence of knee OA stands at 16.0% (95% CI, 14.3%-17.8%), with an incidence rate of 203 per 10,000 person-years (95% CI, 106–331). This degenerative joint disease primarily impacts the knee, causing pain, stiffness, and reduced mobility, which significantly impair the quality of life [5, 9, 12]. The prevalence of knee OA has been steadily increasing due to factors such as aging populations, rising obesity rates, and sedentary lifestyles. Given its widespread impact, there is an urgent need for effective diagnostic tools and treatment strategies to manage this condition better.

Traditionally, knee OA has been assessed using qualitative methods such as the Kellgren-Lawrence (KL) [7] grading system. a widely used tool for classifying the severity of knee OA based on radiographic images. It categorizes knee OA into five grades based on specific radiographic features such as joint space narrowing, osteophyte formation, subchondral sclerosis, and bone deformity. While the KL grading system provides a standardized framework for assessing knee OA, and relies heavily on the subjective visual interpretation of radiographic images by clinicians, that introduces several challenges like variability in diagnosis, inaccuracy, inconsistent treatment plans, lack of precision.

Besides, there are some other challenges to assess the severity level, because of the unavailability of the labeled data, low quality and poor contrast ratio of available X-ray images, etc. To address these challenges [10], our research proposes a novel quantitative methodology for assessing KOA. Our approach leverages advanced image processing techniques, including state-of-the-art edge detection algorithms, optimization methods, and local smoothing techniques, to provide accurate and reproducible measurements of the knee joint space. This methodology aims to overcome the limitations of low-quality X-ray images and the subjective nature of existing detection methods, offering a reliable and efficient tool for knee OA assessment. Our method is designed to be efficient, requiring minimal processing time and computational resources, making it practical for routine use in clinical settings.

This paper has been organized as follows. Section 2 discusses the relevant background studies, Section 3 provides the picture of the problem domain, Section 4 states the proposed methodology in details, 5 provides the results and analysis, and finally, Section 6 summarizes the research contribution.

2 Background Study

This section reviews various methodologies employed in the automated diagnosis and assessment of knee OA, categorizing them based on their objectives and approaches, their performance, and the limitations.

NSysS '25, Sylhet, Bangladesh

ACM ISBN 979-8-4007-2122-9/25/12
https://doi.org/10.1145/3777555.3777566

Kondal et al. [8] developed a two-stage model aimed at automatically grading knee radiographs on the Kellgren-Lawrence (KL) scale using convolutional neural networks (CNNs). The first stage involves an object detection model that segments individual knees from the radiograph. In the second stage, a regression model grades each knee separately on the KL scale. The researchers utilized the Osteoarthritis Initiative (OAI) dataset for initial training and a private dataset from an Indian hospital for fine-tuning. However, here, performance drops without fine-tuning on target datasets, lack of generalizability and the reliance on KL grading is subjective factors that can affect the consistency of the training data.

Antony et al. [3] proposed a *fully convolutional network* (*FCN*) for the automatic localization of knee joints, followed by a CNN for multi-class classification and regression to quantify knee OA severity. The FCN localizes the joints, and the CNN is trained to predict the severity of OA. However, this is computationally costly, and performance heavily that depends on the quality and size of the training datasets, with potential overfitting to specific data characteristics. That may cause severe bias as well.

Tiulpin et al. [13] utilized a deep *Siamese CNN* to classify knee radiographs into KL grades. The network incorporates an attention mechanism to highlight radiological features influencing the network's decisions. Here, despite attention maps, the deep learning model remains as a "black box" and lacks generalization.

Brahim et al. [4] developed a decision support tool for the early detection of knee OA using a combination of image pre-processing and machine learning models. However, their method needs significant domain knowledge, and may not capture all relevant information. Not only that, but inconsistencies can arise in feature extraction and model performance across different datasets.

Heidar et al.[6] presented a deep learning-based method for automatically localizing joint areas on knee radiographs. The approach combines localization with subsequent diagnostic models. Here, potential errors may propagate through multiple stages of processing, and may cause overall complexity and computational requirements. Most of the studies [1, 2, 11] illustrate the diverse approaches to automated knee OA diagnosis and assessment. While deep learning based models offer powerful tools for analysis. However, their dependency on large, high-quality datasets and significant computational resources are considered as notable limitations. The reliance on subjective KL grading introduces variability and potential bias in the training data, highlighting the need for more objective and consistent measurement techniques. Manual feature engineering approaches, although valuable, may not fully capture the complexity of the data and require substantial domain expertise.

3 Problem Domain

The traditional method for assessing knee OA is the Kellgren-Lawrence (KL) grading system. Knee OA is typically detected through X-rays, but X-rays can not store a lot of information, making it very difficult to determine the severity and details of the condition accurately.

While the KL grading system is widely used, it has several limitations:

(1) **Subjectivity**: The system relies heavily on the visual interpretation of radiographic images by clinicians, leading to inter-observer variability and potential inconsistencies in diagnosis.
(2) **Qualitative Nature**: The KL grading system provides a broad categorization of knee OA severity but lacks the granularity needed for detailed assessment and precise monitoring of disease progression.
(3) **Diagnostic Variability**: Different clinicians may interpret the same radiographic features differently, resulting in variability in the assigned KL grades and affecting the reliability of the grading system.

Given these limitations, there is a pressing need for objective, quantitative methods that can provide consistent and precise measurements of knee OA severity from radiographic images.

By developing quantitative methods that utilize advanced image processing algorithms and machine learning techniques, we can achieve accurate and reproducible measurements of key radiographic features. Specifically, measuring the *knee joint space*—the gap between the tibia and femur bones—has emerged as a critical parameter in evaluating the severity of OA.

3.1 Dataset

Our study utilizes two primary datasets: one obtained from a publicly available source and another generated through our image processing pipeline.

Open Dataset- This is the primary dataset that has been collected from a publicly available source, specifically from the Kaggle platform. This dataset consists of knee X-ray images that have been graded according to the *Kellgren-Lawrence* (*KL*) grading system. The KL grading system categorizes knee osteoarthritis (OA) severity into five distinct grades based on specific radiographic features. The distribution of images across these grades is as follows:
Grade 0, 1, and 2: Each grade contains 1000 images, *Grade 3*: Contains 750 images and *Grade 4*: Contains 150 images. All images in this dataset are in grayscale and have a resolution of 224 x 224 pixels. The grayscale nature of these images presents a challenge in accurately detecting and measuring knee gaps due to the varying contrast and quality of the X-rays.
Generated Dataset: To enhance the accuracy and reliability of our measurements, we have generated a secondary dataset using advanced image processing techniques. We have employed the Fast-SAM image segmentation algorithm to process the grayscale X-ray images from the primary dataset. *FastSAM,* known for its efficiency and precision, was used to segment the images and detect the knee gaps, resulting in a new set of images with enhanced features.

The FastSAM method [14] produces segmented images in RGB format, which facilitates more accurate detection of knee gaps. The segmentation process involved identifying the boundaries of the tibia and femur bones, which are crucial for measuring the knee joint space. This new dataset, generated through our preprocessing pipeline, provided a more detailed and precise representation of the knee joint structure, enabling more accurate measurements of the knee gaps.

3.2 Data Processing

The processing steps for generating the secondary dataset included:

- **Image Segmentation**: The grayscale X-ray images were processed using the FastSAM algorithm to segment the knee joint and identify the boundaries of the tibia and femur bones.
- **Image Conversion**: The segmented images were converted from grayscale to RGB format to enhance the detection accuracy.
- **Knee Gap Measurement**: The segmented images were analyzed to measure the knee gaps, providing quantitative data on the knee joint space.

Leveraging both the publicly available dataset and the generated dataset, our study aims to address the limitations of traditional KL grading, and provides a more objective and quantitative method for assessing knee OA severity. This comprehensive approach combines the strengths of existing data with advanced image processing techniques to improve the accuracy and reliability of knee gap measurements, ultimately contributing to better diagnostic and treatment strategies for knee OA.

4 Proposed Methodology

In this section, we provide problem formulation and the details.

4.1 Problem Formulation

The problem of KOA assessment can be formulated as a regression task where the goal is to predict a continuous score representing the severity of OA from knee radiographs. The key steps involved in this process include:

(1) **Image Pre-processing:** Enhancing the quality of knee radiographs is crucial to facilitate accurate edge detection and joint space measurement. This step involves techniques such as *Gaussian Blurring* to reduce noise and adaptive thresholding to enhance the contrast of edges in the image. By preprocessing the images, we ensure that, the subsequent edge detection algorithms can operate on higher quality, more distinct images.

(2) **Edge Detection:** The next step is to identify the edges of the tibia and femur bones using advanced edge detection algorithms. In our approach, we utilize a combination of Sobel and FastSAM edge detection techniques. The Sobel operator highlights intensity gradients in the image, which correspond to the edges of the bones. FastSAM, although not specifically trained on X-ray images, is adapted to detect object boundaries effectively. The combination of these techniques allows for a more robust edge detection process, crucial for accurate joint space measurement.

(3) **Joint Space Measurement:** After detecting the edges of the tibia and femur bones, we calculate the distance between these edges to quantify the knee joint space. This measurement is a critical indicator of the severity of knee OA, as the narrowing of the joint space is a hallmark of the disease. By applying simulated annealing and local smoothing techniques, we refine the edge detection results to ensure precise joint space measurements. This step provides the quantitative data needed to assess the progression of knee OA.

(4) **Severity Prediction:** Instead of using machine learning models to predict OA severity based on the measured joint space, we focus on a more direct quantitative analysis. By measuring the percentage shrinkage of the joint space, we can predict the grade of the KL based on these quantitative measurements. This approach provides a clear, objective metric to evaluate the severity of knee OA, reducing the subjectivity associated with traditional methods. The severity of OA is measured in terms of the percentage reduction in joint space, allowing for a more precise assessment of disease progression.

4.2 Detail Steps

Our approach for knee OA assessment using image processing techniques is described in detail as follows.

4.2.1 Image Preprocessing. The initial step involves enhancing the quality of knee radiographs to facilitate accurate edge detection and joint space measurement.

- **Applying Sobel Operator:** The Sobel operator has been applied to the X-ray images to highlight edges and create clearer images for further processing.
- **Generating Dataset for FastSAM:** The enhanced images have been then used to generate a dataset suitable for the FastSAM segmentation algorithm.

Algorithm 1 Applying Sobel for Edge Detection on Original Dataset

Require: Image *img*
Ensure: Sobel magnitude image *sobel_mag*

```
sobel_x ← Sobel in x-direction
sobel_y ← Sobel in y-direction
sobel_mag ← √(sobel_x² + sobel_y²)
sobel_mag ← Normalize to 0-255 scale
return sobel_mag
```

$$sobel\_mag \leftarrow \sqrt{sobel\_x^2 + sobel\_y^2}$$

4.2.2 Edge Detection. We utilize the advanced edge detection algorithms on the segmented images generated by FastSAM.

- **Preprocessing RGB Image:** We enhance edges by applying Gaussian blur and adaptive thresholding to each channel of the RGB image.
  - **Gaussian Blur:** This reduces noise in the image by averaging the pixel values with their neighbors.
  - **Adaptive Thresholding:** This converts the image to binary form by setting pixel values above a certain threshold to 255 (white) and below to 0 (black). It adapts to different lighting conditions in the image.
  - **Morphological Operations:** Operations like closing and opening help in removing small noise and closing small holes in the detected edges.
- **Detect Combined Edges:** We combine edges detected in each channel using bitwise operations.

Algorithm 2 Pre-processing RGB Image

Require: RGB Image *img*
Ensure: Combined edge-detected image
Split *img* into channels
for each channel **do**
  Apply Gaussian blur
  Apply adaptive thresholding
  Apply morphological operations
  Detect edges using Canny
  Append edges to list
end for
Combine edges from all channels
return combined edges

4.2.3 Finding Initial Edges. We identify the initial edges of the tibia and femur bones using the preprocessed images.

- **Detect Upper and Lower Edges:** Iterate through columns of the image and detect the upper and lower edges based on intensity values. For each column, we start from the top (for the upper edge) and bottom (for the lower edge) of the image and move towards the center, looking for significant changes in intensity that indicate the presence of an edge.

Algorithm 3 Find Initial Edges

Require: Image *img*, Interval *interval*, Step *step*, Gap *gap*
Ensure: Upper and lower edge arrays
Preprocess *img* to detect edges
Initialize edge arrays
for each column in *img* **do**
  Detect upper edge
  Detect lower edge
end for
return upper and lower edge arrays

4.2.4 Simulated Annealing. To refine the detected edges, we have applied simulated annealing, which optimizes the edge positions for accuracy.

- **Initial Temperature:** Start with a high temperature to allow significant changes in edge positions.
- **Cooling Schedule:** Gradually reduce the temperature to limit the changes and focus on fine-tuning the edge positions.
- **Cost Function:** Calculate the cost based on the difference between the current and new edge positions. Accept new positions if the cost is lower or with a certain probability if the cost is higher.

Algorithm 4 Simulated Annealing

Require: Edge positions *edges*, Parameters *params*
Ensure: Optimized edges
Initialize temperature *temp*
while *temp* > threshold **do**
  for each edge point **do**
    Generate new position
    Calculate cost
    if new cost is better **then**
      Update edge position
    else
      Accept with a probability
    end if
  end for
  Reduce temperature
end while
return optimized edges

4.2.5 Local Smoothing. We further smooth the detected edges using a moving average filter to remove any noise and irregularities.

Algorithm 5 Local Smoothing

Require: Edge array *edges*, Window size *window_size*
Ensure: Smoothed edges
Apply moving average filter to *edges*
return smoothed edges

We process all images in the dataset to detect and refine the edges, and calculate the joint space.

Algorithm 6 Process All Images

Require: Input folder *input_folder*
Ensure: Edge detection results and joint space calculations
for each image in *input_folder* **do**
  Preprocess and detect edges
  Apply simulated annealing
  Smooth edges
  Calculate joint space
  Save results to CSV files
end for

4.2.6 Joint Space Calculation. We calculate the joint space by measuring the distance between the upper and lower edges detected.

Algorithm 7 Calculation of Joint Space

Require: Upper edge *upper_edge*, Lower edge *lower_edge*
Ensure: Joint space *joint_space*
$joint\_space = lower\_edge - upper\_edge$
return *joint_space*

4.2.7 Processing Pipeline for New Images. When a new X-ray image is received, the processing pipeline involves the following steps:

- **Image Pre-processing:**
  - Applying Sobel operator to enhance edges.
  - Converting to RGB format for FastSAM.
- **Edge Detection:**
  - Using FastSAM to segment the image.
  - Applying Canny edge detection to detect combined edges.
- **Refinement:**
  - Using simulated annealing to optimize edge positions.
  - Smoothing the edges using local smoothing techniques.
- **Joint Space Measurement:**
  - Measuring the distance between the upper and lower edges to calculate the joint space.
  - Calculating the shrinkage percentage relative to the maximum shrinkage observed in grade 4 images.
- **Prediction:**
  - Based on the calculated shrinkage percentage, prediction of the KL grade for the new image.

5 Results and Analysis

In this section, we provide the results and the relevant analysis.

5.1 Testbed Description

The testing environment for our experiments involved Google Colab, providing free access to GPUs (such as NVIDIA Tesla T4, P4, or P100) and TPUs. We have also used Kaggle Kernels: Part of Kaggle's platform, Kaggle Kernels provides AMD EPYC or Intel Xeon CPUs, along with GPUs like NVIDIA Tesla P100 or T4. It supports both Python and R languages, offers up to 16 GB of RAM, and enables collaborative data analysis through shared notebooks and datasets of Kaggle.

We have used pre-trained segmentation model FastSAM for generating segmented dataset. Additionally, we used CV, a collection of algorithms for image processing and computer vision (CV), as well as the libraries associated with Google Colab, the cloud-based platform for statistical data analysis, and Visual Studio Code, which is widely used for Python development.

5.2 Edge Detection

Our model successfully detected the edges by first performing segmentation of the image, then applying an algorithm that includes smoothing and simulated annealing for local refinement. This process ensured high precision in edge detection a visual representation of which can be seen in Figure 1

Our algorithm very accurately detected the upper and lower edges, crucial for the subsequent steps in osteoarthritis detection.

5.3 Joint Space Computation

We have determined the coordinates of multiple points along both the upper and lower edges of the knee joint. By calculating the distance between these corresponding points, we obtained precise measurements of the joint space width. Subsequently, we filtered out the regions of interest (ROIs) to focus on the most relevant sections for osteoarthritis detection. Specifically, we isolated the joint space widths in the left and right parts of the joint. These

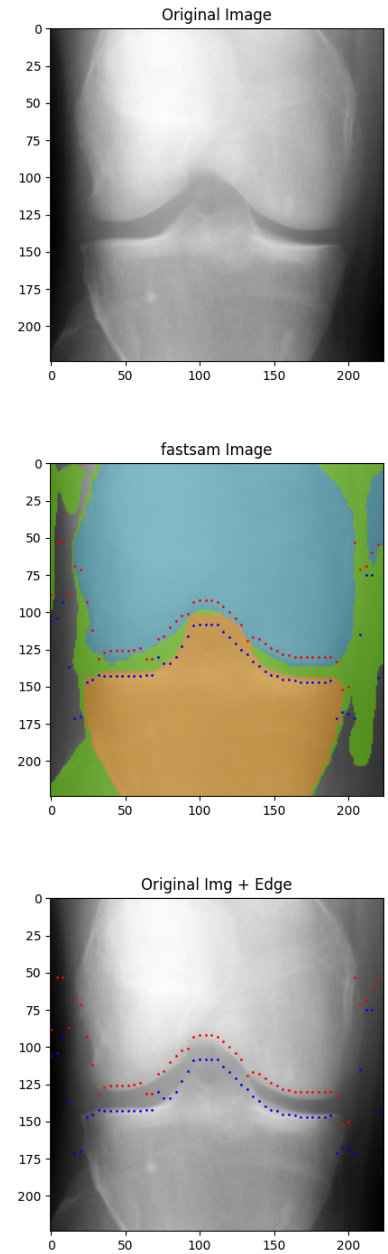

Figure 1: Detected upper edge and lower edge of the knee joint

measurements were then used for further statistical analysis. For each image, we calculated the joint space width by averaging the distances within the ROIs. Next, we performed a comprehensive statistical analysis of the joint space widths across all images within each grade, calculating key metrics such as the mode, mean, and standard deviation for both the left and right gaps. This rigorous

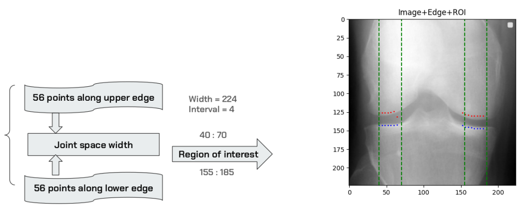

Figure 2: Illustration of edges and *Regions of Interest* (*ROI*)

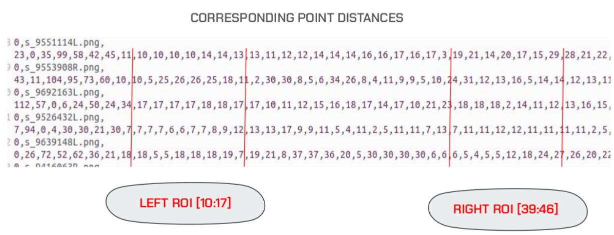

Figure 3: Point distances with *Left* and *Right ROI* markings

approach allowed us to accurately characterize the joint space widths for different grades of osteoarthritis.

5.3.1 Joint Space Width per Image. The joint space width for each image was determined through a detailed process:

(1) At first, we have identified the y-coordinates of 56 points along the upper and lower edges of the knee joint in 224-pixel images, spaced at 4-pixel intervals.
(2) Next, we have calculated the distances between corresponding points along the upper and lower edges to establish the joint space.
(3) We have then filtered out the left region of interest (ROI) from pixel index 40 to 70 (corresponding to points 10 to 17 out of 56) and the right ROI from pixel index 155 to 185 (points 39 to 46).
(4) Scaling the values within these ROIs allowed us to identify the most frequently occurring value (mode), which represents the joint space width for both the left and right sides of the joint in each image.

Figure 2 visually represents the process, showing the identified points along the upper and lower edges, the calculation of point distances, and the delineation of the left and right ROIs.

Figure 3 illustrates the point distances for all 56 points in the images, with the left and right ROIs marked accordingly.

The table (Table 1) illustrates similarities and frequent occurrences of values in both the left and right Regions of Interest (ROI), derived from knee joint edge point distances.

After calculating the distances between points along the upper and lower edges and filtering out the regions of interest (ROI), the values were scaled, and the mode was calculated as the left and right joint space widths. The table 2 presents these measurements for several images.

Table 1: *Left* and *Right ROI* values for images

Image	Left ROI								Right ROI							
Number	10	11	12	13	14	15	16	17	39	40	41	42	43	44	45	46
1	18	18	18	19	7	19	21	8	22	22	22	22	22	22	51	60
2	11	11	11	9	9	4	7	7	7	6	6	6	7	9	8	9
3	11	11	11	11	11	11	12	12	11	11	11	2	10	11	19	28
4	12	12	12	19	19	18	12	12	16	13	11	8	11	8	7	7

Table 2: *Joint Space Width* for some selected images

Image_ID	Grade	Left Joint Space Width	Right Joint Space Width
9865771R	0	18	15
9176441R	1	15	15
9761503R	2	15	12
9914944L	3	12	12
9568974L	4	9	12
9528886L	0	18	18

Table 3: Joint Space Width statistics for different grades

Grade	Mode Left	Mean Left	Std Dev Left	Mode Right	Mean Right	Std Dev Right
0	18	18.91	2.58	18	18.88	2.42
1	18	15.94	2.87	18	16.32	2.84
2	15	14.30	4.07	15	14.45	3.76
3	12	11.80	4.01	12	12.68	2.41
4	12	11.38	4.71	12	11.73	4.82

5.3.2 Joint Space Width per Grade. For each grade, we performed a statistical analysis on the joint space widths obtained from all images of that grade. This analysis involved several key steps:

1. Through statistical analysis, we identified the most probable value of joint space width in the left and right regions of the knee joint for each grade.

2. We calculated the mode, mean, and standard deviation for both the left and right gaps, providing a comprehensive understanding of the joint space characteristics for each grade.

3. Additionally, we computed the percentage joint space width, which normalizes the joint space width relative to the overall joint size, offering a clearer perspective on joint space variations across different grades.

To visualize the distribution of joint space widths, we plotted the distributions for the left and right joint spaces separately for each grade. After denoising the data, we combined the distributions into a single image. The figures 4 illustrate the distribution plots for each grade.

The figure 4 shows the distribution plots of the joint space widths for the left and right regions separately, as well as the combined denoised plots for each grade. The images illustrate the similarity and multiple occurrences of values in the joint space widths across different grades.

The table 3 summarizes the joint space width statistics for various grades.

Finally, by analyzing the mode, mean, and standard deviation for each grade from Table 3, we determined a standard value of left and right joint space for each grade. This joint space width was

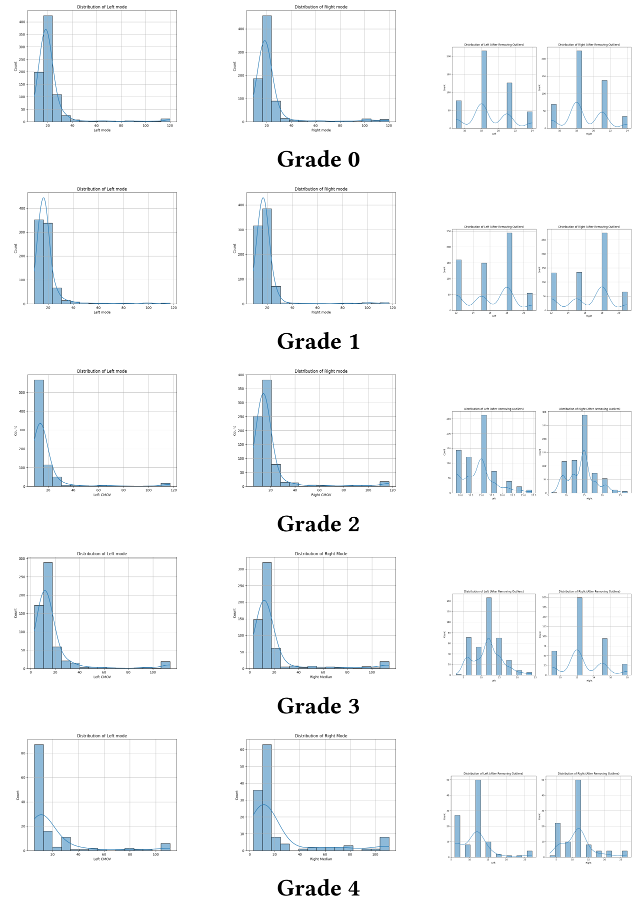

Figure 4: Distribution of *Joint Space Width* for different KL grades

Table 4: The width of joint space for different grades.

Grade	Joint Space Width (px)		Joint Space Width (%)	
	Left	Right	Left	Right
0	19	19	8.0	8.0
1	16	16	7.0	7.0
2	14	14	6.0	6.0
3	11	12	5.0	5.0
4	11	11	5.0	5.0

also expressed as a percentage of the total image height, which is 224 pixels. The table 4 presents these values.

Variation in joint space widths across different grades, as shown in Table 4 is crucial for understanding the role of joint space narrowing in detecting and assessing the severity of osteoarthritis.

5.4 Joint Space Analysis

Our analysis reveals that joint space width is a significant indicator in detecting osteoarthritis. Images with a joint space width of less than 7% of the image height (224 pixels) are typically identified as osteoarthritic. This threshold corresponds predominantly to Grades 4 and 3, and occasionally to Grade 2. Conversely, images with joint space widths greater than 7% are usually classified as non-osteoarthritic, corresponding to Grades 0 and 1, and sometimes Grade 2.

Optimum Range for Osteoarthritis Detection:

- Images from Grades 3 and 4 consistently exhibit osteoarthritis.
- Grade 2 images with narrowed joint space are often osteoarthritic.
- Joint space width below 7% of the total image height (224 pixels) is a reliable marker for osteoarthritis.

Therefore, if a knee joint under diagnosis exhibits a joint space width of less than 7%, it can be inferred that the joint is affected by osteoarthritis.

Joint Space Width < 7%	Joint Space Width ≥ 7%

The validity of this discovery has been rigorously tested, ensuring robustness and reliability. Performance metrics are detailed in the subsequent section to further substantiate these findings.

The testing process involved evaluating images from the test dataset using our algorithm. Each image underwent segmentation and edge detection, followed by measurement of left and right joint spaces. If joint space width was under 7% (for images from folders 0, 1, or 2), or over 7% (for folders 2, 3, or 4), osteoarthritis was predicted; otherwise, it was not. Results were recorded for accuracy assessment against actual diagnoses, ensuring our algorithm's effectiveness in osteoarthritis detection.

We have used the following metrics for performance measure.
Accuracy per Grade: Bar charts showing the accuracy achieved for each grade of osteoarthritis in Table 5

Table 5: Accuracy per KL grade

Grade	Total	Correct	Accuracy (%)
0	92	78	84.78
1	96	73	76.04
2	98	98	100.0
3	94	67	71.28
4	25	20	80.0

5.5 Performance Analysis

Performance metrics were computed to quantitatively assess the algorithm's effectiveness:

- **Specificity:** The proportion of true negative results among the actual negatives.
- **Sensitivity/Recall:** The proportion of true positive results among the predicted positives.
- **F1 Score:** The harmonic mean of precision and recall.
- **Overall Accuracy:** The ratio of correctly predicted images to the total number of images tested.

The performance metrics table (Table 6) summarizes key evaluation metrics for the algorithm. Specificity and Sensitivity/Recall indicate balanced detection capabilities, with Specificity at 74%

Table 6: Output of performance metrics

Metric	Value (%)
Specificity	74
Sensitivity/Recall	73
F1 Score	62
Overall Accuracy	82.96

highlighting accurate negative predictions. The F1 Score of 62% reflects moderate precision and recall balance, crucial for classification tasks. Overall Accuracy at 82.96% underscores the algorithm's effectiveness across all predictions, demonstrating robust performance across varied conditions.

6 Conclusions

Our contribution lies in developing an efficient, low-resource system that eliminates the need for labeled data in edge detection and model training. This approach enables rapid pre-diagnosis, saving significant time and computational resources.

Efficient Low Resource System: Our approach eliminates the need for labeled data in edge detection and model training, significantly reducing computational requirements.

Pre-Diagnosis Potential: By leveraging minimal resources and rapid computation, our method offers the potential to expedite pre-diagnosis processes, saving valuable time and costs.

In this study, we measured the joint space between the tibia and femur for each grade of osteoarthritis. By identifying the percentage range of joint space width for osteoarthritic knee joints, we developed a method to aid in decision-making for advanced diagnosis and treatment. The proposed framework achieved an accuracy of 82.96% in osteoarthritis detection, demonstrating its efficiency and suitability for low-resource clinical settings.

References

[1] Rafique Ahmed and Ali Shariq Imran. 2024. Knee Osteoarthritis Analysis Using Deep Learning and XAI on X-Rays. *IEEE Access* 12 (2024), 68870–68879. https://doi.org/10.1109/ACCESS.2024.3400987

[2] Sozan Mohammed Ahmed and Ramadhan J. Mstafa. 2022. Identifying Severity Grading of Knee Osteoarthritis from X-ray Images Using an Efficient Mixture of Deep Learning and Machine Learning Models. *Diagnostics* 12, 12 (2022). https://doi.org/10.3390/diagnostics12122939

[3] Joseph Antony, Kevin McGuinness, Kieran Moran, and Noel E. O'Connor. 2017. Automatic Detection of Knee Joints and Quantification of Knee Osteoarthritis Severity Using Convolutional Neural Networks. *Springer International Publishing* 1, 1 (2017), 376–390.

[4] Amine Brahim, Rachid Jennane, Redouane Riad, Thierry Janvier, Lamine Khedher, Hakim Toumi, and Eric Lespessailles. 2019. A Decision Support Tool for Early Detection of Knee Osteoarthritis Using X-ray Imaging and Machine Learning: Data from the Osteoarthritis Initiative. *Computerized Medical Imaging and Graphics* 73 (2019), 11–18.

[5] Mohammad Ziaul Haider, Rijwan Bhuiyan, Shamim Ahmed, Ahmad Zahid-Al-Quadir, Minhaj Rahim Choudhury, Syed Atiqul Haq, and Mohammad Mostafa Zaman. 2022. Risk factors of knee osteoarthritis in Bangladeshi adults: a national survey. *BMC Musculoskeletal Disorders* 23, 1 (2022), 1–9.

[6] Behzad Heidar. 2011. Knee Osteoarthritis Prevalence, Risk Factors, Pathogenesis and Features: Part I. *Caspian Journal of Internal Medicine* 2, 2 (2011), 205–212.

[7] Michael D. Kohn, Andrew A. Sassoon, and Nathan D. Fernando. 2016. Classifications in Brief: Kellgren-Lawrence Classification of Osteoarthritis. *Clinical Orthopaedics and Related Research* 474, 8 (2016), 1886–1893.

[8] Sudeep Kondal, Viraj Kulkarni, Ashrika Gaikwad, Amit Kharat, and Aniruddha Pant. 2020. Automatic Grading of Knee Osteoarthritis on the Kellgren-Lawrence Scale from Radiographs Using Convolutional Neural Networks. *eess.IV* 1, 1 (2020), 1–6.

[9] Elena Losina, A. Paltiel, Alexander Weinstein, Edward Yelin, David Hunter, Stephanie Chen, Kristina Klara, Lisa Suter, Daniel Solomon, Sara Burbine, Rochelle Walensky, and Jeffrey Katz. 2014. Lifetime Medical Costs of Knee Osteoarthritis Management in the United States: Impact of Extending Indications for Total Knee Arthroplasty. *Arthritis Care & Research* 67 (07 2014). https://doi.org/10.1002/acr.22412

[10] T. Paixao, M.D. DiFranco, R. Ljuhar, D. Ljuhar, C. Goetz, Z. Bertalan, H.P. Dimai, and S. Nehrer. 2020. A novel quantitative metric for joint space width: data from the Osteoarthritis Initiative (OAI). *Osteoarthritis and Cartilage* 28, 8 (2020), 1055–1061. https://doi.org/10.1016/j.joca.2020.04.003

[11] Lior Shamir, Shao Min Ling, William W Scott Jr, Adam Bos, Nikita Orlov, Tomasz J Macura, David M Eckley, Luigi Ferrucci, and Ilya G Goldberg. 2009. Knee x-ray image analysis method for automated detection of osteoarthritis. *IEEE Transactions on Biomedical Engineering* 56, 2 (February 2009), 407–415. https://doi.org/10.1109/TBME.2008.2006025

[12] Jaimie D Steinmetz, Garland T Culbreth, Lydia M Haile, Quinn Rafferty, Justin Lo, Kai Glenn Fukutaki, Jessica A Cruz, Amanda E Smith, Stein Emil Vollset, Peter M Brooks, et al. 2023. Global, regional, and national burden of osteoarthritis, 1990–2020 and projections to 2050: a systematic analysis for the Global Burden of Disease Study 2021. *The Lancet Rheumatology* 5, 9 (2023), e508–e522.

[13] Aleksandr Tiulpin, Johan Thevenot, Esa Rahtu, Pekka Lehenkari, and Simo Saarakkala. 2018. Automatic Knee Osteoarthritis Diagnosis from Plain Radiographs: A Deep Learning-Based Approach. *Scientific Reports* 8, 1 (2018), 1727.

[14] Xu Zhao, Wenchao Ding, Yongqi An, Yinglong Du, Tao Yu, Min Li, Ming Tang, and Jinqiao Wang. 2023. Fast Segment Anything. (2023).